

# An integrated biochemical system for nitrate assimilation and nitric oxide detoxification in *Bradyrhizobium japonicum*

Juan J. Cabrera\*, Ana Salas\*, María J. Torres\*, Eulogio J. Bedmar\*, David J. Richardson†‡, Andrew J. Gates†‡<sup>1</sup> and María J. Delgado\*<sup>1</sup>

\*Estación Experimental del Zaidín, CSIC, PO Box 419, Granada 18080, Spain

†Centre for Molecular and Structural Biochemistry, University of East Anglia, Norwich Research Park, Norwich NR4 7TJ, U.K.

‡School of Biological Sciences, University of East Anglia, Norwich Research Park, Norwich NR4 7TJ, U.K.

Rhizobia are recognized to establish N<sub>2</sub>-fixing symbiotic interactions with legume plants. *Bradyrhizobium japonicum*, the symbiont of soybeans, can denitrify and grow under free-living conditions with nitrate (NO<sub>3</sub><sup>-</sup>) or nitrite (NO<sub>2</sub><sup>-</sup>) as sole nitrogen source. Unlike related bacteria that assimilate NO<sub>3</sub><sup>-</sup>, genes encoding the assimilatory NO<sub>3</sub><sup>-</sup> reductase (*nasC*) and NO<sub>2</sub><sup>-</sup> reductase (*nirA*) in *B. japonicum* are located at distinct chromosomal loci. The *nasC* gene is located with genes encoding an ABC-type NO<sub>3</sub><sup>-</sup> transporter, a major facilitator family NO<sub>3</sub><sup>-</sup>/NO<sub>2</sub><sup>-</sup> transporter (NarK), flavoprotein (Flp) and single-domain haemoglobin (termed Bjgb). However, *nirA* clusters with genes for a NO<sub>3</sub><sup>-</sup>/NO<sub>2</sub><sup>-</sup>-responsive regulator (NasS-NasT). In the present study, we demonstrate NasC and NirA are both key

for NO<sub>3</sub><sup>-</sup> assimilation and that growth with NO<sub>3</sub><sup>-</sup>, but not NO<sub>2</sub><sup>-</sup> requires *flp*, implying Flp may function as electron donor to NasC. In addition, *bjgb* and *flp* encode a nitric oxide (NO) detoxification system that functions to mitigate cytotoxic NO formed as a by-product of NO<sub>3</sub><sup>-</sup> assimilation. Additional experiments reveal NasT is required for NO<sub>3</sub><sup>-</sup>-responsive expression of the *narK-bjgb-flp-nasC* transcriptional unit and the *nirA* gene and that NasS is also involved in the regulatory control of this novel bipartite assimilatory NO<sub>3</sub><sup>-</sup>/NO<sub>2</sub><sup>-</sup> reductase pathway.

**Key words:** bacterial denitrification, bacterial haemoglobin, nitrate reduction, nitric oxide reductase, nitrite reduction.

## INTRODUCTION

Fixation of atmospheric dinitrogen (N<sub>2</sub>) by plant-associated symbiotic soil bacteria, collectively termed rhizobia, is a significant agricultural process that reduces dependence on synthetic nitrogen (N) containing fertilizers in crop production. This protects water quality and human health as well as the wider environment. In addition to N<sub>2</sub> fixation, the soybean endosymbiont *Bradyrhizobium japonicum* USDA110 is capable of growing anaerobically with the water-soluble nitrate (NO<sub>3</sub><sup>-</sup>) anion, as an alternative terminal electron acceptor to oxygen (O<sub>2</sub>), which is reduced to N<sub>2</sub> gas by respiratory denitrification. During this process, several free N-containing intermediates are produced, including: (i) the oxanylon nitrite (NO<sub>2</sub><sup>-</sup>), (ii) the gaseous cytotoxic free-radical nitric oxide (NO) and (iii) the potent and long-lived greenhouse gas nitrous oxide (N<sub>2</sub>O). In *B. japonicum*, the denitrification apparatus is encoded by the *napEDABC*, *nirK*, *norCBQD* and *nosRZDFYLX* genes, which express the periplasmic NO<sub>3</sub><sup>-</sup> reductase (NapABC), copper-containing NO<sub>2</sub><sup>-</sup> reductase (NirK), cytochrome-*c* NO reductase (NorCB) and N<sub>2</sub>O reductase (NosZ) enzymes, respectively [1]. This bacterium is distinguished by the ability to denitrify under both free-living and symbiotic conditions [2–4].

Several reports suggest that rhizobial denitrification is the main driver for production and release of the environmentally damaging agents NO and N<sub>2</sub>O from alfalfa and soybean nodules [5–8]. NO is a highly reactive and well-studied ozone-depleting agent, whereas N<sub>2</sub>O is increasingly recognized as a powerful greenhouse gas with an estimated 300-fold higher radiative potential for

global warming, molecule for molecule, compared with carbon dioxide [9–11]. Importantly, in active root nodules, NO also acts as a potent inhibitor of nitrogenase, the central enzyme of symbiotic N<sub>2</sub>-fixation [8,12]. Under free-living denitrifying conditions, the *B. japonicum* proteins NirK and NorCB are physiologically important for the synthesis and detoxification of NO, respectively [1]. However, several studies suggest the involvement of other sinks for NO that are distinct from the recognized denitrification pathway in nodules [8,13]. For example, in related bacteria, NO may be oxidized to NO<sub>3</sub><sup>-</sup> or reduced to N<sub>2</sub>O by cytoplasmic detoxification enzymes. These systems include single-domain haemoglobins (sdHbs), truncated haemoglobins (trHbs), flavohaemoglobins (FHbs) and flavorubredoxin (FIRD) [14–18].

Following sequencing of the *B. japonicum* USDA110 genome [19], several studies have investigated the involvement of a putative bacterial sdHb, termed Bjgb, in NO-detoxification, under free-living conditions [3,20]. This bacterial haemoglobin is encoded by the ORF blr2807 and resides within a cluster of other uncharacterized ORFs (blr2803–09) predicted to encode components of a NO<sub>3</sub><sup>-</sup> assimilation (Nas) pathway, including: an ABC-type NO<sub>3</sub><sup>-</sup> transport system (blr2803–05), a major facilitator superfamily (MFS)-type NO<sub>3</sub><sup>-</sup>/NO<sub>2</sub><sup>-</sup> transporter (blr2806), an FAD-dependent NAD(P)H oxidoreductase (blr2808) and the catalytic subunit of the assimilatory NO<sub>3</sub><sup>-</sup> reductase (blr2809), termed NasC (we note the gene for the assimilatory NO<sub>3</sub><sup>-</sup> reductase in *B. japonicum* was previously termed *nasA*, but here we unify the gene nomenclature for  $\alpha$ -proteobacteria). The genome also contains a putative

Abbreviations: Bjgb, *Bradyrhizobium japonicum* haemoglobin; FHb, flavohaemoglobin; Flp, flavoprotein; FIRD, flavorubredoxin; MFS, major facilitator superfamily; MV-NIR, methyl viologen-dependent nitrite reductase; MV-NR, methyl viologen-dependent nitrate reductase; NapABC, periplasmic respiratory quinol/nitrate oxidoreductase; NarK, nitrate/nitrite transporter; Nas, assimilatory nitrate reductase; NirA, assimilatory nitrite reductase; NirK, copper-dependent respiratory nitrite reductase; NorCB, cytochrome-*c* nitric oxide reductase; NosZ, nitrous oxide reductase; PSY, peptone-salts-yeast extract; sdHb, single-domain haemoglobin; SNP, sodium nitroprusside; WT, wild-type;  $\mu_{max}$  (app), apparent maximum growth rate.

<sup>1</sup> Correspondence may be addressed to either of these authors (email a.gates@uea.ac.uk or mariajesus.delgado@eez.csic.es).

ferredoxin-dependent assimilatory  $\text{NO}_2^-$  reductase (NirA) that is present at bl14571, a distinct locus on the chromosome. This putative *nirA* gene lies immediately downstream of genes recently reported to code for a  $\text{NO}_3^-/\text{NO}_2^-$  responsive regulatory system (NasS-NasT), similar to that characterized in the model  $\text{NO}_3^-$ -utilizing soil bacterium *Paracoccus denitrificans* PD1222 [21,22]. However, to date, a role for the proteins encoded at blr2803–09 and bl14571–73 loci in  $\text{NO}_3^-/\text{NO}_2^-$  assimilation and conceivably NO management in *B. japonicum* remains to be established.

Although the biochemical components for Nas systems may be highly modular, in related  $\alpha$ -proteobacteria such as *P. denitrificans* and *Rhodobacter capsulatus* E1F1, genes encoding regulatory and structural elements for the  $\text{NO}_3^-$  assimilation pathway are typically found together [23,24]. For example, in *P. denitrificans*, the genes required for import and reduction of  $\text{NO}_3^-$  and/or  $\text{NO}_2^-$  are encoded by *nasABGHC* and the *nasTS* genes required for  $\text{NO}_3^-/\text{NO}_2^-$ -responsive regulatory control are found immediately upstream [25]. Here, the assimilatory  $\text{NO}_3^-/\text{NO}_2^-$  reductase apparatus includes a:  $\text{NO}_3^-/\text{NO}_2^-$  transporter (NasA),  $\text{NO}_2^-$  reductase (NasB), ferredoxin (NasG),  $\text{NO}_2^-$  transporter (NasH) and  $\text{NO}_3^-$  reductase (NasC). Notably, the *nasG* gene is highly conserved in  $\text{NO}_3^-/\text{NO}_2^-$  assimilation gene clusters, which is consistent with a key role for the NasG ferredoxin in mediating electron flux from the NADH-oxidizing site in NasB to the sites of  $\text{NO}_3^-$  and  $\text{NO}_2^-$  reduction in NasC and NasB respectively, in order to prevent intracellular accumulation of  $\text{NO}_2^-$  [25]. In *P. denitrificans*, the RNA-binding protein NasT has been recently shown to positively and directly regulate *nas* expression (i.e. *nasABGHC*) by interacting with the *nasA*-leader mRNA. The  $\text{NO}_3^-/\text{NO}_2^-$ -binding sensor NasS controls NasT activity and the NasS and NasT proteins co-purify as a stable heterotetrameric regulatory complex, NasS-NasT in the absence of inducer [21]. The NasS-NasT system from *B. japonicum* has now been characterized by Sánchez et al. [22] and shown to regulate expression of *napE* and *nosZ* genes for the dissimilatory denitrification pathway.

The processes and enzymes for rhizobial denitrification have been well studied [1–4]; however, the biochemical apparatus for  $\text{NO}_3^-/\text{NO}_2^-$  assimilation by plant-associated rhizobia has yet to be characterized. In the present work, we demonstrate a dual role for the blr2806–09 and bl14571–73 loci for  $\text{NO}_3^-/\text{NO}_2^-$  assimilation and NO management in *B. japonicum*.

## EXPERIMENTAL

### Bacterial strains, plasmids and growth conditions

The bacterial strains and plasmids used in the present study are listed in Supplementary Table S1. Gene deletion and transcriptional reporter construction used previously established methods [26,27], with key modifications as outlined below. *B. japonicum* strains were grown routinely under aerobic conditions at 30 °C in peptone-salts-yeast extract (PSY) medium supplemented with 0.1 % (w/v) L-arabinose [28]. Growth curves for different N-sources were performed in Bergersen minimal medium [29] supplemented with 10 mM  $\text{KNO}_3$  (BN3), 1 mM  $\text{NaNO}_2$  (BN2) or 10 mM  $\text{KNO}_3$  plus 6.5 mM L-glutamate (BGN3) as sole N-sources and incubated aerobically or anaerobically. Anaerobic conditions were reached by incubating the cells in completely filled glass serum tubes. Growth was followed by measuring attenuation (*D*) of cell cultures at 600 nm.

To test growth inhibition by nitrosative stress, cells were grown in Bergersen minimal medium with 6.5 mM L-glutamate (BG) as sole N-source and incubated under microaerobic conditions in serum tubes sealed with rubber septa. The headspace of these

tubes was filled with a gas mixture of 2 % (v/v)  $\text{O}_2$  and 98 % (v/v)  $\text{N}_2$  and was replaced with fresh gas mixture every 24 h. Nitrosative stress was induced by adding 1 mM sodium nitroprusside (SNP) or spermine NONOate to the cultures 24 h after inoculation. To test cell survival after nitrosative stress induction, cells were grown to early stationary growth phase under the same conditions as for growth inhibition experiments (final *D* value at 600 nm was  $\sim 0.5$ ). Then, 1 mM SNP or spermine NONOate was added to the cultures (replica cultures were not subjected to nitrosative stress as controls). Cell cultures were incubated at 30 °C and 0.1 ml of samples were taken periodically, serially diluted in growth medium and plated into PSY-agar. Colonies were counted after incubation for 7 days under aerobic conditions. The capacity for colony formation of control cells was considered as 100 % survival.

To induce the expression of NorCB as a cellular marker for NO, *B. japonicum* was grown in Bergersen minimal medium where glycerol was replaced with 10 mM succinate as carbon source (BS) [30,31]. The medium was supplemented with 10 mM  $\text{KNO}_3$  as sole N-source (BSN3). In these experiments, the headspace was filled with 2 % (v/v)  $\text{O}_2$  and 98 %  $\text{N}_2$  (v/v). In contrast with microaerobic growth conditions, the atmosphere for cultures was not replaced. As such, cells consumed the  $\text{O}_2$  present and reached anoxic conditions after 24 h incubation.

Antibiotics were added to *B. japonicum* cultures at the following concentrations ( $\mu\text{g}\cdot\text{ml}^{-1}$ ): chloramphenicol 20, tetracycline 100, spectinomycin 200, streptomycin 200 and kanamycin 200. *Escherichia coli* strains were cultured in LB medium [32] at 37 °C including tetracycline 10, spectinomycin 20, streptomycin 20, kanamycin 30 and ampicillin at 200  $\mu\text{g}\cdot\text{ml}^{-1}$ . *E. coli* S17-1 served as the donor for conjugative plasmid transfer [33].

### Construction of *B. japonicum narK-lacZ* and *nirA-lacZ* transcriptional fusions

For construction of transcriptional fusion reporter plasmids, DNA fragments for the *narK* (520 bp) and *nirA* (563 bp) promoter regions were amplified using primers *narK-lacZ\_For/narK-lacZ\_Rev* and *nirA-lacZ\_For/nirA-lacZ\_Rev*, respectively (see Supplementary Table S2 for oligonucleotide sequences). Fragments were digested with PstI or PstI-EcoRI and cloned into the *lacZ* fusion vector pSUP3535, which is derived from pSUP202 [33] to give plasmids pDB4009 and pDB4018 respectively (Supplementary Table S1). The correct orientation of cloned inserts was verified by sequencing.

Transcriptional fusion plasmids pDB4009 and pDB4018 were integrated by homologous recombination into the chromosome of wild-type (WT) *B. japonicum* USDA110 and *nasS* and *nasT* mutants to produce strains 4009, 4012–4009, 4013–4009, 4018, 4012–4018 and 4013–4018 detailed in Supplementary Table S1. Correct recombination was checked by PCR analysis of genomic DNA isolated from each strain.

### Growth conditions for $\beta$ -galactosidase activity assay of *narK-lacZ*, *nirA-lacZ* and *norC-lacZ* fusions

Strains 4009, 4012–4009, 4013–4009, 4018, 4012–4018 and 4013–4018 containing the *narK-lacZ* or *nirA-lacZ* reporter-fusion constructs (Supplementary Table S1) were grown aerobically in PSY medium. Cells were harvested by centrifugation at 8000 *g* for 10 min, washed twice with nitrogen-free Bergersen medium and cultured aerobically in the same medium or in BN3 medium, for 48 h (until a *D* value of  $\sim 0.5$  at 600 nm was obtained). To measure  $\beta$ -galactosidase activity from the *norC-lacZ* fusion,

plasmid pRJ2499 (Supplementary Table S1) was integrated by homologous recombination into the chromosome of *bjgb*, *nasC*, *napA* and *nasC*, *napA* mutants to produce strains 4001-2499, 4003-2499, GRPA1-2499 and GRPA1-4003-2499 respectively (Supplementary Table S1). In order to induce expression of *nor* genes, cells were cultured in BSN3 medium with 2% (v/v) initial O<sub>2</sub> concentration.

### Construction and complementation of *B. japonicum* mutants

Genomic and plasmid DNA isolation was carried out using the REALPURE Genomic DNA purification Kit (Real) and Qiagen Plasmid Kit (Qiagen) respectively. Custom oligonucleotide primers were supplied by Sigma, PCR was performed using the High Fidelity DNA polymerase Phusion enzyme (Thermo) and DNA digestions were carried out using Fast digest enzymes (Fermentas). All mutants constructed in the present work were made by in frame deletion of the corresponding gene using the mobilizable pK18*mobsacB* suicide vector that conferred kanamycin resistance and sucrose sensitivity on the host (Supplementary Table S1). To generate mutant strains, upstream and downstream regions of relevant target genes were amplified by PCR using the gene-specific primer sets detailed in Supplementary Table S2.

For the *narK* deletion mutant, upstream (834 bp) and downstream (981 bp) DNA fragments flanking *blr2806* were amplified by PCR using *blr2806\_up\_For/blr2806\_up\_Rev* and *blr2806\_down\_For/blr2806\_down\_Rev* primer pairs (Supplementary Table S2). The 981-bp fragment was inserted into pK18*mobsacB* as an XbaI-HindIII fragment that contained a new unique XhoI restriction site immediately downstream of the XbaI site. Subsequently, the 834-bp fragment was inserted into this plasmid as a BamHI-XhoI fragment yielding plasmid pDB4000. Double recombination of pDB4000 with the *B. japonicum* genome led to the replacement of the WT *blr2806* gene encoding a 459 amino acid (aa) protein for an in frame truncated version encoding 38 aa.

To generate *bjgb* and *nasT* deletion mutants, upstream and downstream regions flanking *blr2807* (824 and 884 bp fragments) and *blI4573* (696 and 736 bp fragments) were amplified by PCR using gene-specific primer pairs, i.e. *blr2807\_up\_For/blr2807\_up\_Rev* and *blr2807\_down\_For/blr2807\_down\_Rev* for *blr2807* and *blI4573\_up\_For/blI4573\_up\_Rev* and *blI4573\_down\_For/blI4573\_down\_Rev* for *blI4573* (Supplementary Table S2). The PCR products containing the upstream regions of *blr2807* and *blI4573* were inserted separately into pK18*mobsacB* as EcoRI-XbaI fragments and subsequently the downstream PCR products were inserted into the respective plasmids as XbaI-HindIII DNA fragments yielding plasmids pDB4001 and pDB4013 (Supplementary Table S1). Double recombination of pDB4001 and pDB4013 with the *B. japonicum* genome led to the replacement of the *blr2807* gene encoding a 142 aa protein and the *blI4573* gene encoding a 196 aa protein with in-frame truncated versions of 33- and 27-aa for *blr2807* or *blI4573*, respectively.

To generate the *flp* and *nasC* mutants, upstream and downstream regions of *blr2808* (983 and 856 bp) and *blr2809* (829 and 840 bp) were amplified by PCR using gene-specific primer pairs *blr2808\_up\_For/blr2808\_up\_Rev* and *blr2808\_down\_For/blr2808\_down\_Rev* for *blr2808* and *blI2809\_up\_For/blI2809\_up\_Rev* and *blI2809\_down\_For/blI2809\_down\_Rev* for *blI2809* (Supplementary Table S2). The PCR product containing the upstream regions of *blr2808* and *blr2809* were cloned into separate pK18*mobsacB* plasmids as EcoRI-BamHI fragments and subsequently the downstream DNA

regions were inserted into the relevant plasmid as BamHI-HindIII fragments to give pDB4002 and pDB4003. Double recombination of either pDB4002 or pDB4003 with the *B. japonicum* genome led to the replacement of the *blr2808* gene (encoding a 418-aa protein) or the *blr2809* gene (encoding a 901-aa protein) for in-frame truncated versions encoding a 37- or 27-aa peptide respectively.

The *ntrABC* mutant was generated by double recombination of *B. japonicum* USDA110 genomic DNA with plasmid pDB4004 (Supplementary Table S1). To generate pDB4004, the upstream region of *blr2803* (773 bp) and the downstream region of *blr2805* (721 bp) were amplified by PCR using primer pairs *blr2803\_up\_For/blr2803\_up\_Rev* and *blr2805\_down\_For/blr2805\_down\_Rev* (Supplementary Table S2). Firstly, the PCR product containing the upstream region was digested with BamHI and XbaI restriction enzymes and cloned into pK18*mobsacB*. Then, the PCR product corresponding to the downstream region was inserted into the plasmid as an XbaI-PstI fragment to give plasmid pDB4004 (Supplementary Table S1). Double recombination of pDB4004 with the *B. japonicum* genome replaced *blr2803–05* genes for an in-frame truncated version encoding a 31-aa peptide.

The *nirA* and *nasS* mutants were generated by double recombination of *B. japonicum* USDA110 genomic DNA with plasmids pDB4011 and pDB4012 respectively. To generate pDB4011 and pDB4012, the upstream and downstream regions of *blI4571* (641 and 692 bp) and *blI4572* (687 and 664 bp) were amplified by PCR using the primer pairs *blI4571\_up\_For/blI4571\_up\_Rev* and *blI4571\_down\_For/blI4571\_down\_Rev* for *blI4571* and *blI4572\_up\_For/blI4572\_up\_Rev* and *blI4572\_down\_For/blI4572\_down\_Rev* for *blI4572* (Supplementary Table S2). PCR products containing the upstream regions were cloned first into pK18*mobsacB* as EcoRI-KpnI DNA fragments. Then, amplified downstream regions were inserted into the plasmid as KpnI-XbaI fragments yielding plasmids pDB4011 and pDB4012 (Supplementary Table S1). Finally, double recombination replaced *blI4571* and *blI4572* genes (encoding 625- and 388-aa proteins respectively) for in-frame truncated versions encoding 17- and 23-aa peptides respectively.

All plasmids constructed for mutagenesis were sequenced and transferred via conjugation into *B. japonicum* USDA110 using *E. coli* S17-1 as donor strain. Double recombination events were favoured by first selecting single recombinants for kanamycin resistance and screening candidates by PCR. Then, selected clones containing the plasmid co-integrated in the genome were grown in PSY-agar medium supplemented with sucrose 10% (w/v) to select for double recombinants. Sucrose resistant colonies were checked for kanamycin sensitivity. Double recombinants were confirmed by PCR.

*B. japonicum* GRC131-4001 containing a double mutation in *bjgb* and *norC* was generated by transferring plasmid pJNOR43M2 [34] via conjugation into the *B. japonicum* *bjgb* mutant (Supplementary Table S1). Double recombinants were selected for kanamycin resistance and tetracycline sensitivity. The correct replacement of the WT *norC* gene by kanamycin resistance gene (*aphII*) insertion was checked by PCR.

*B. japonicum* GRPA1-4003 containing a double mutation in *napA* and *nasC* was generated by transferring plasmid pBG602Ω [26] via conjugation into the *B. japonicum* *nasC* mutant (Supplementary Table S1) using *E. coli* S17-1 as donor strain. Double recombination events were favoured by growth on agar plates containing sucrose. Mutant strains resistant to spectinomycin/streptomycin, but sensitive to kanamycin were checked by PCR for correct replacement of the WT fragment by the Ω interposon.

The *bjgb*, *flp* and *nasC* strains were complemented with pDB4014, pDB4015, pDB4017 expression constructs containing the corresponding intact genes (Supplementary Table S1). For this, *bjgb*, *flp* and *nasC* genes were amplified by PCR using primer sets blr2807\_For/blr2707\_Rev, blr2808\_For/blr2808\_Rev and blr2809\_For/blr2809\_Rev (Supplementary Table S2). DNA fragments containing the relevant ORF and Shine–Dalgarno sequence were cloned separately into pTE3 vector [35]. All complementation constructs were sequenced and transferred via conjugation into the relevant *B. japonicum* mutant using *E. coli* S17-1 as donor strain. Complemented strains 4001-pDB4014, 4002-pDB4015 and 4003-pDB4017 (Supplementary Table S1) were confirmed by plasmid extraction and checked by restriction analyses and PCR.

### Analysis of gene expression by RT-PCR

Total RNA was isolated from *B. japonicum* cells grown anaerobically to a *D* of  $\sim 0.4$  (at 600 nm) in BN3 medium, as previously described [36]. First strand cDNA synthesis was performed with the SuperScript II reverse transcriptase (Invitrogen) according to the supplier's guidelines, using 1  $\mu$ g of total RNA and primer e (Supplementary Table S2). cDNA generated was used for amplification of putative intergenic regions between blr2805 and blr2809, using primers pairs a1/a2 to d1/d2 (Supplementary Table S2), essentially as described by Sambrook and Russell [32]. In negative controls, reverse transcriptase was omitted and for positive controls PCR was performed with *B. japonicum* USDA110 genomic DNA as template.

### $\beta$ -Galactosidase assays

$\beta$ -Galactosidase activity was determined using permeabilized cells from at least three independently grown cultures assayed in triplicate for each strain and condition, as previously described [37]. The absorbance data at 420 and 600 nm were determined for all samples and cultures in a plate reader (SUNRISE Absorbance Reader, TECAN), using the software XFluor4 (TECAN) and specific activities were calculated in Miller units.

### Determination of $\text{NO}_3^-$ reductase and $\text{NO}_2^-$ reductase activity

*B. japonicum* was grown under aerobic conditions in PSY medium, harvested by centrifugation at 8000 *g* for 10 min at 4 °C, washed twice with BN3 medium and inoculated to a *D* value of  $\sim 0.4$  (at 600 nm) in fresh minimal medium of the same composition. Following 72 h incubation under relevant conditions, cells were harvested, washed with 50 mM Tris/HCl buffer (pH 7.5) to remove excess  $\text{NO}_2^-$  and then resuspended in 1 ml of the same buffer prior to assay for enzymatic activity. Methyl viologen-dependent  $\text{NO}_3^-$  reductase (MV-NR) and  $\text{NO}_2^-$  reductase (MV-NIR) activity was measured essentially as described by Delgado et al. [26]. The reaction mixture contained 50 mM Tris/HCl buffer (pH 7.5), 200  $\mu$ M MV, 100  $\mu$ l of cell suspension (with 0.02–0.04 mg of protein) and 10 mM  $\text{KNO}_3$  or 100  $\mu$ M  $\text{NaNO}_2$  for MV-NR or MV-NIR activity respectively. Methyl viologen was reduced by the addition of freshly prepared sodium dithionite (dissolved in 300 mM  $\text{NaHCO}_3$  solution) at a final concentration of 14.4 mM.

### Haem-staining analysis

Aerobically grown *B. japonicum* cells were harvested by centrifugation, washed twice with BSN3 medium and resuspended in 500 ml of fresh medium of the same composition. Microaerobic conditions were then established with 2% (v/v)

initial  $\text{O}_2$  concentration and cells were cultured for 48 h until a final *D* of  $\sim 0.5$  (at 600 nm) was reached. Cells were disrupted using a French pressure cell (SLM Aminco, Jessup) and membranes were isolated as described previously [26]. Membrane protein aliquots were diluted in sample buffer [124 mM Tris/HCl, pH 7.0, 20% (v/v) glycerol, 5% (v/v) SDS and 50 mM 2-mercaptoethanol] and incubated at room temperature for 10 min. Membrane proteins were separated at 4 °C by SDS-PAGE [12% (w/v) acrylamide resolving gel with 20  $\mu$ g of protein per lane], transferred to a nitrocellulose membrane and stained for haem-dependent peroxidase activity [38], using the chemiluminescence detection kit 'SuperSignal' (Pierce, Thermo Fisher Scientific). Protein concentration was estimated using the Bio-Rad assay (Bio-Rad Laboratories).

### Intracellular $\text{NO}_2^-$ determination

*B. japonicum* cells were harvested, washed and lysed by using a French pressure cell (SLM Aminco, Jessup). Soluble cell extracts were prepared by centrifugation at 10000 *g* for 30 min at 4 °C and assayed for  $\text{NO}_2^-$  using the method of Nicholas and Nason [39].

### NO consumption activity

NO consumption rates were determined using intact *B. japonicum* cells [obtained from BSN3 cultures with 2% (v/v) initial  $\text{O}_2$  and a *D* of  $\sim 0.5$  (at 600 nm)] with a 2 mm ISONOP NO electrode APOLLO 4000<sup>®</sup> (World Precision Institute). The reaction chamber (2 ml) was temperature-controlled, magnetically stirred and contained: 760  $\mu$ l of 25 mM phosphate buffer (pH 7.4), 900  $\mu$ l of cell suspension (4–5 mg protein), 100  $\mu$ l of an enzyme mix containing *Aspergillus niger* glucose oxidase (40 units·ml<sup>-1</sup>) and bovine liver catalase (250 units·ml<sup>-1</sup>) (Sigma-Aldrich), 90  $\mu$ l of 1 M sodium succinate and 100  $\mu$ l of 320 mM glucose. Once a steady base line was obtained, 50  $\mu$ l of a saturated NO solution (1.91 mM at 20 °C) was added to the cuvette to start the reaction. Each assay was monitored until the NO detection had dropped to zero, i.e. when all NO was consumed.

### $\text{N}_2\text{O}$ measurements

*B. japonicum* cells were cultured as indicated above for NO consumption experiments, except that in addition to 2% (v/v) initial  $\text{O}_2$ , the headspace of the cultures also contained 10% (v/v) acetylene in order to inhibit  $\text{N}_2\text{O}$  reductase activity. After 96 h growth, gaseous samples were taken from the headspace of cultures.  $\text{N}_2\text{O}$  was measured using an HP 4890D gas chromatography instrument equipped with an electron capture detector (ECD). The column was packed with Porapak Q 80/100 MESH and the carrier gas was  $\text{N}_2$  at a flow rate of 23 ml·min<sup>-1</sup>. The injector, column and detector temperatures were 125, 60 and 375 °C respectively. The samples were injected manually using a Hamilton<sup>®</sup> Gastight syringe. Peaks corresponding to  $\text{N}_2\text{O}$  were integrated using GC ChemStation Software (Agilent Technologies<sup>®</sup>) and the concentrations of  $\text{N}_2\text{O}$  in each sample were calculated using  $\text{N}_2\text{O}$  standards (Air Liquid).

## RESULTS

### Genetic basis for $\text{NO}_3^-$ and $\text{NO}_2^-$ assimilation in endosymbiotic denitrifying rhizobia

*B. japonicum* USDA110 contains a putative assimilatory  $\text{NO}_3^-$  reductase encoded at blr2809 (Figure 1A) [19,20]. Experiments confirmed that *B. japonicum* is able to grow aerobically or anaerobically using  $\text{NO}_3^-$  as sole N-source with values for  $\mu_{\text{max}}$

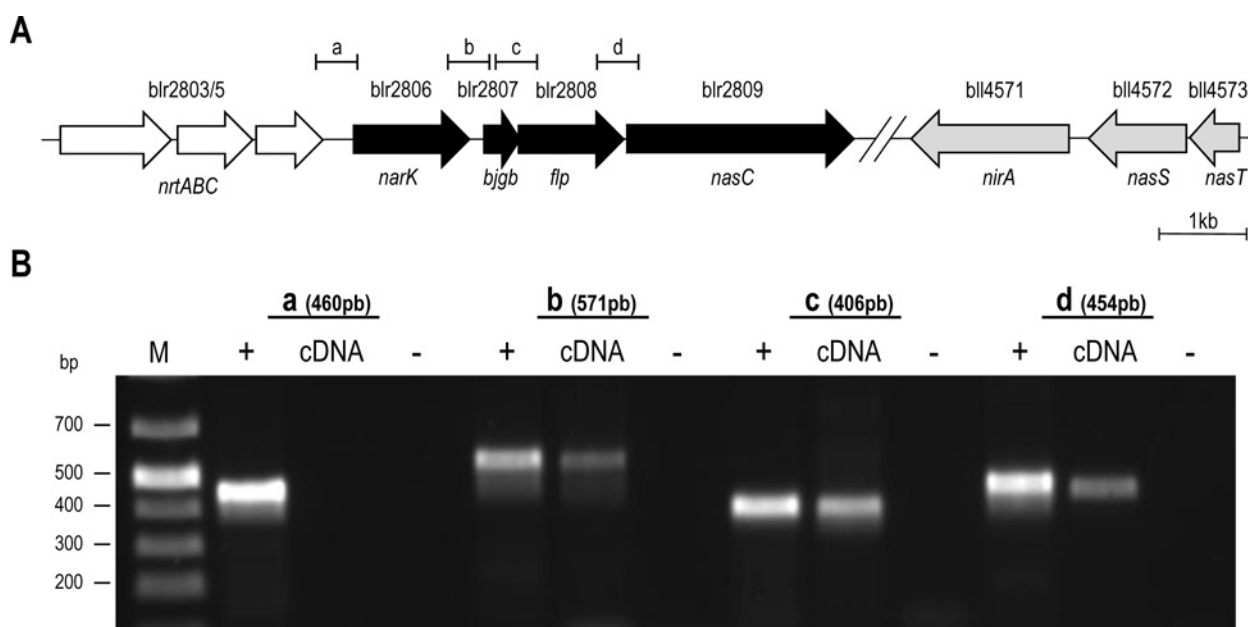


**Figure 1** Organization of regulatory and structural genes for the assimilatory  $\text{NO}_3^-/\text{NO}_2^-$  reductase pathway in *B. japonicum*

(A) Schematic representation of the *blr2803-5*, *blr2806-09* and *bli4571-73* ORFs investigated in the present study. Putative intergenic regions probed by RT-PCR to determine the transcriptional architecture of the *blr2806-09* region (i.e. *nark-bjgb-flp-nasC*) are labelled a–d. (B) The results for RT-PCR analysis obtained by agarose gel electrophoresis for regions a–d. Total RNA isolated from cells grown anaerobically with  $\text{NO}_3^-$  served as the template for cDNA synthesis, whereas PCR amplifications using genomic DNA and without reverse transcriptase enzyme served as positive and negative controls respectively (as indicated above lanes).

(app) (apparent maximum growth rate) of approximately 0.06 and  $0.04 \text{ h}^{-1}$  respectively (Figures 2A and 2B; Supplementary Table S3).

Notably, *blr2809* lies downstream of several putative ORFs with predicted roles in N-metabolism (Figure 1A). To investigate the transcriptional architecture of this region, RT-PCR experiments were performed to detect intergenic regions (a–d). Here, specific cDNA was obtained for all regions except ‘a’ (Figure 1B). These findings reveal that *blr2806–09* constitute a transcriptional unit. Thus, in-frame deletion strategies for subsequent molecular genetics experiments were adopted to prevent possible polar effects on co-transcribed genes (see ‘Experimental’ section for details).

Analysis of the amino acid sequence of *blr2809* suggests the protein is a member of the molybdenum bis-molybdopterin dinucleotide cofactor binding superfamily and contains consensus motifs for co-ordination of an N-terminal [4Fe-4S] cluster and a C-terminal [2Fe-2S] cluster. This general organization is similar to other assimilatory  $\text{NO}_3^-$  reductases, including *P. denitrificans* NasC and *Klebsiella oxytoca* NasA from the  $\alpha$ - and  $\gamma$ -proteobacterial clades, respectively [25]. Accordingly, we adopt the  $\alpha$ -proteobacterial nomenclature, NasC, for the *B. japonicum* protein encoded at *blr2809* hereafter. A *B. japonicum* strain that was mutated by in-frame deletion of *nasC* lost the capacity for aerobic or anaerobic growth with  $\text{NO}_3^-$  as sole N-source (Figures 2A and 2B; Supplementary Table S3). However, this strain retained the ability to grow using  $\text{NO}_2^-$  as sole N-source and displayed similar growth kinetics to WT [ $\mu_{\text{max}}$  (app)  $\sim 0.03 \text{ h}^{-1}$ ] (Figure 3A; Supplementary Table S3).

The genome of *B. japonicum* also contains an ORF for a putative assimilatory  $\text{NO}_2^-$  reductase (*nirA*) at *bli4571*, a distinct locus situated  $\sim 2 \text{ Mb}$  from *nasC* on the chromosome (Figure 1A). NirA contains canonical cysteine-rich motifs in central and C-terminal sequence regions for iron–sulfur co-

ordination and formation of the sirohaem  $\text{NO}_2^-$  reductase/sulfite reductase ferredoxin half-domain respectively. However, NirA lacks N-terminal FAD- and NAD(P)H-binding domains present in bacterial NirB-type NAD(P)H-dependent  $\text{NO}_2^-$  reductases [25]. Deletion of *nirA* resulted in *B. japonicum* being unable to grow aerobically or anaerobically with either  $\text{NO}_3^-$  or  $\text{NO}_2^-$  as sole N-source (Figures 2A, 2B and 3A; Supplementary Table S3). The ability of WT and *nirA* cells to consume 1 mM  $\text{NO}_2^-$  during incubation experiments was tested (Figure 3B, open symbols). Whereas all  $\text{NO}_2^-$  was removed from minimal medium after  $\sim 6$  days by WT cells, no significant decrease in extracellular  $\text{NO}_2^-$  was observed in *nirA* mutant cultures (Figure 3B). Conversely,  $\text{NO}_2^-$  production experiments using 10 mM  $\text{NO}_3^-$ , as sole N-source, revealed that WT cells did not accumulate  $\text{NO}_2^-$  in the extracellular medium (Figure 3B, closed symbols). However, accumulation of  $\sim 1 \text{ mM}$   $\text{NO}_2^-$  was observed following incubation of the *nirA* mutant with  $\text{NO}_3^-$  (Figure 3B). Thus, pre-cultured cells of the *nirA* mutant retained the capacity to reduce  $\text{NO}_3^-$  to  $\text{NO}_2^-$ , but no further.

The putative flavoprotein (Flp), encoded at *blr2808*, contains canonical FAD- and NAD(P)H-binding domains typical of cytoplasmic NAD(P)H-dependent oxidoreductases present in several bacterial Nas operons [23] and is a strong candidate for mediating electron transfer to NasC and/or NirA. A *B. japonicum flp* mutant was unable to grow aerobically or anaerobically with  $\text{NO}_3^-$  as the sole N-source (Figures 2A and 2B; Supplementary Table S3). However, the *flp* mutant displayed similar growth kinetics and yields [ $\mu_{\text{max}}$  (app)  $\sim 0.03 \text{ h}^{-1}$ , maximum  $D$  (at 600 nm) =  $0.43 \pm 0.08$ ] to that observed for WT [ $\mu_{\text{max}}$  (app)  $\sim 0.03 \text{ h}^{-1}$ , maximum  $D$  (at 600 nm) =  $0.51 \pm 0.01$ ] when cultured aerobically with  $\text{NO}_2^-$  (Figure 3A; Supplementary Table S3). These findings suggest that Flp mediates electron transfer to NasC, but not to NirA. In order to confirm that deletion of *flp* did not influence expression

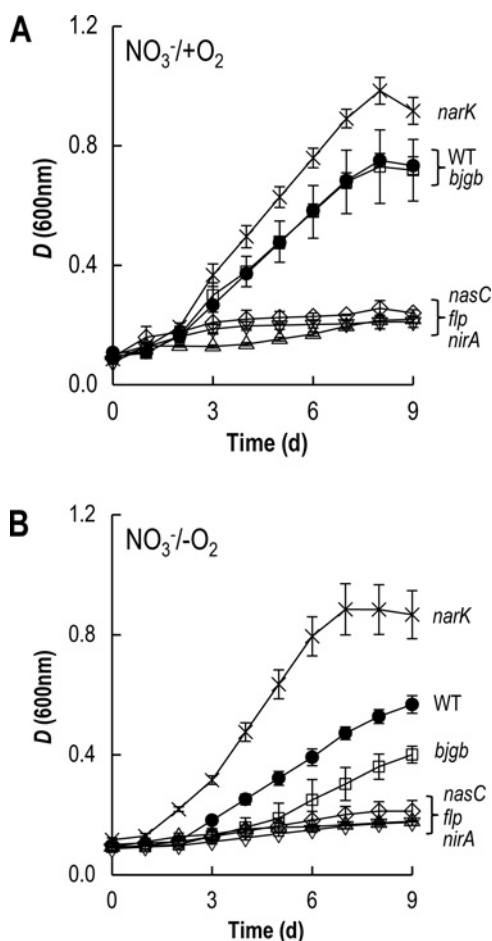


**Figure 2**  $\text{NO}_3^-$ -dependent growth of *B. japonicum*

Growth curves for WT (●), *narK* (×), *bjgb* (□), *flp* (▽), *nasC* (◇) and *nirA* (△) strains were measured under aerobic (A) and anaerobic (B) conditions in BN3 minimal medium with  $\text{NO}_3^-$  as sole N-source. The results presented are the mean of two biological replicates assayed in triplicate.

of downstream genes, relevant strains were complemented with either pDB4017 (*nasC*) or pDB4015 (*flp*) constructs. The presence of pDB4017 and pDB4015 plasmids restored both aerobic and anaerobic growth of the *nasC* and *flp* mutants in the presence of  $\text{NO}_3^-$  to near WT levels, thereby verifying the phenotypes observed (Supplementary Table S3).

Deletion of the *blr2803–05* ORFs, predicted to encode an NrtABC-type  $\text{NO}_3^-$  transporter, did not affect the capacity of the cells to grow with  $\text{NO}_3^-$  as sole N-source (Supplementary Table S3). Bioinformatics analysis of *blr2806* revealed that it encodes a putative member of the MFS of membrane proteins, sharing 66% and 59% amino acid similarity with the  $\text{NO}_3^- / \text{NO}_2^-$  antiporters *E. coli* NarK [40] and *P. denitrificans* NarK2 [41] respectively (Supplementary Figure S1). Thus, we term this MFS-type transporter NarK rather than the generic ‘nitrite extrusion protein’ genome annotation currently assigned (<http://genome.kazusa.or.jp/rhizobase/>).

*A. B. japonicum narK* mutant showed improved growth kinetics and yields when cultured aerobically [ $\mu_{\text{max}}$  (app)  $\sim 0.09 \text{ h}^{-1}$ , maximum  $D$  (at 600 nm)  $= 0.98 \pm 0.05$ ] or anaerobically [ $\mu_{\text{max}}$  (app)  $\sim 0.07 \text{ h}^{-1}$ , maximum  $D$  (at 600 nm)  $= 0.89 \pm 0.09$ ] with  $\text{NO}_3^-$  as sole N-source when compared with aerobic [ $\mu_{\text{max}}$  (app)  $\sim 0.06 \text{ h}^{-1}$ , maximum  $D$  (at 600 nm)  $= 0.73 \pm 0.12$ ] or anaerobic [ $\mu_{\text{max}}$  (app)  $\sim 0.04 \text{ h}^{-1}$ , maximum  $D$  (at 600 nm)  $= 0.61 \pm 0.03$ ]

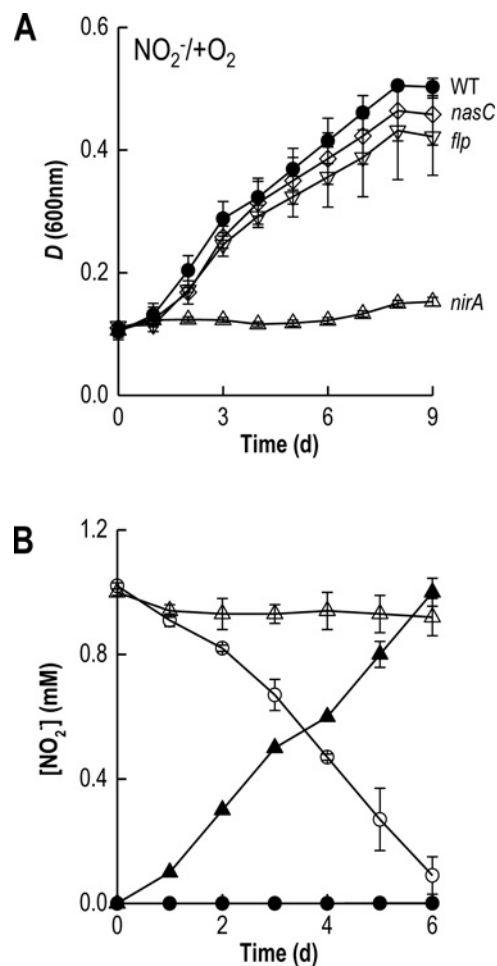


**Figure 3**  $\text{NO}_2^-$ -dependent growth of *B. japonicum*

(A) Growth curves for WT (●), *flp* (▽), *nasC* (◇) and *nirA* (△) strains were measured under aerobic conditions in BN2 minimal medium with  $\text{NO}_2^-$  as sole N-source. (B) Extracellular  $\text{NO}_2^-$  consumption (open symbols) and accumulation (solid symbols), using 1 mM  $\text{NO}_2^-$  or 10 mM  $\text{NO}_3^-$  as sole N-source respectively measured during growth of WT (circles) and *nirA* (triangles) strains. The results presented are the mean of two biological replicates assayed in triplicate.

growth of WT under the same conditions (Figures 2A and 2B; Supplementary Table S3). Furthermore, following 24 h aerobic growth, the *narK* mutant accumulated  $\sim 2$ -fold higher levels of intracellular  $\text{NO}_2^-$  than that accumulated by WT cells, i.e.,  $5.3 \pm 0.7$  compared with  $2.2 \pm 0.1 \text{ nmol NO}_2^- \text{ mg-protein}^{-1}$  for the *narK* and WT strains respectively (Supplementary Figure S2). The addition of L-glutamate to minimal growth medium restored the inability of the *nasC*, *nirA* and *flp* mutants to grow with  $\text{NO}_3^-$  under aerobic or anaerobic conditions (Supplementary Table S3). Under these conditions, growth yields obtained from the *narK* mutant were also similar to those obtained from WT cells (Supplementary Table S3). Collectively, these results confirm the importance of NarK, Flp, NasC and NirA for  $\text{NO}_3^-$  assimilation by *B. japonicum*.

The regulatory proteins encoded by *blI4573* (*nasT*) and *blI4572* (*nasS*) constitute a  $\text{NO}_3^- / \text{NO}_2^-$  responsive two-component system, NasS-NasT, which has been recently reported in *B. japonicum* [22]. A *B. japonicum nasT* mutant strain showed significant growth attenuation compared with the WT cells when cultured aerobically with either  $\text{NO}_3^-$  (Figure 4A; Supplementary

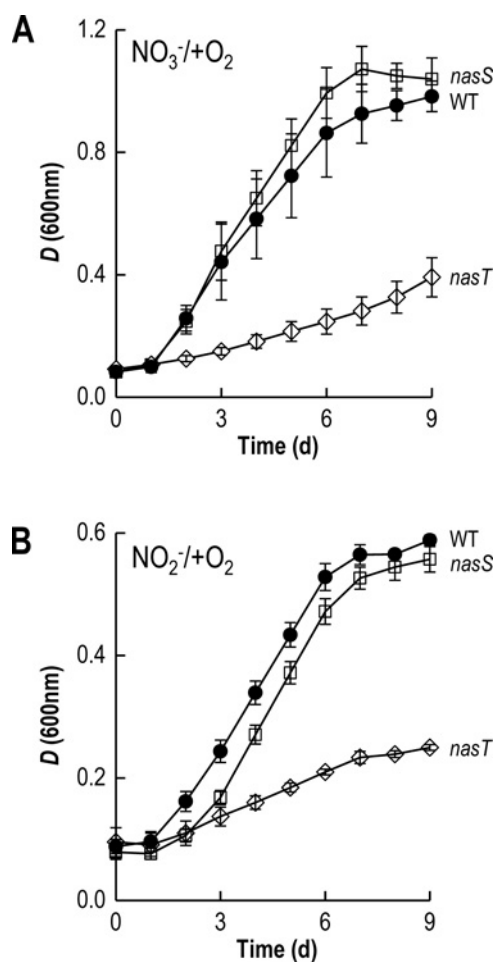


**Figure 4** Growth curves for the *B. japonicum* *nasS* and *nasT* mutants

Growth of WT (●), *nasS* (□) and *nasT* (◇) strains was measured in minimal medium, under aerobic conditions, with either  $\text{NO}_3^-$  (A) or  $\text{NO}_2^-$  (B), as sole N-source. The results presented are the mean of two biological replicates assayed in triplicate.

Table S3) or  $\text{NO}_2^-$  (Figure 4B; Supplementary Table S3) as sole N-source, but growth of this strain was unaffected when cells were grown in the presence of L-glutamate (Supplementary Table S3). By contrast, a strain in which the *nasS* gene was mutated did not show a clear growth defect with respect to WT (Figure 4; Supplementary Table S3).

### A biochemical pathway for assimilation of $\text{NO}_3^-$ and $\text{NO}_2^-$

The biochemical basis of growth phenotypes observed for the various deletion strains was examined by enzymatic activity assay of whole cells, using dithionite-reduced methyl viologen, as an artificial electron donor. Here, MV-NR and MV-NIR activities were measured in WT and *nasC*, *nirA*, *flp*, *bjgb* and *narK* mutants, following aerobic incubation with  $\text{NO}_3^-$  as sole N-source (Table 1). Since *B. japonicum* has periplasmic respiratory  $\text{NO}_3^-$  reductase (NapABC) and  $\text{NO}_2^-$  reductase (NirK) systems that might also use methyl viologen as an electron donor [26,42], control experiments using *napA* and *nirK* mutants were also performed in the present study. Importantly, and as expected, the respective MV-NR and MV-NIR activity levels observed in *napA* and *nirK* cells were similar to those observed in WT cells (Table 1), indicating that the contribution of the NapABC or NirK respiratory enzymes was not significant in cells

**Table 1** MV-NR and MV-NIR activities of *B. japonicum* strains incubated aerobically in minimal medium with  $\text{NO}_3^-$  as sole N-source

<i>B. japonicum</i> str.	Genotype	Activities	
		MV-NR*	MV-NIR†
USDA 110	WT	32.0 ± 5.2	6.9 ± 0.9
GRPA1	<i>napA</i>	32.1 ± 0.5	–
GRK308	<i>nirK</i>	–	7.5 ± 0.8
4003	<i>nasC</i>	n.d.	7.2 ± 1.2
4003-pDB4017	<i>nasC</i> (pDB4017)	30.5 ± 4.8	–
4011	<i>nirA</i>	49.7 ± 1.8	n.d.
4002	<i>flp</i>	68.3 ± 6.7	6.1 ± 0.8
4001	<i>bjgb</i>	28.4 ± 5.0	6.1 ± 0.4
4000	<i>narK</i>	35.8 ± 2.2	10.9 ± 1.5

\*MV-NR and †MV-NIR activities are expressed as nanomoles of  $\text{NO}_2^-$  produced or consumed  $\text{min}^{-1} \cdot \text{mg} \cdot \text{protein}^{-1}$ . Data are expressed as the mean value ± S.D. from at least two different cultures assayed in triplicate; –, not determined; n.d., not detectable.

cultured under aerobic conditions. This provided a solid platform for subsequent experiments.

Significantly, MV-NR activity was not detectable in *nasC* cells, but a similar level of MV-NIR activity was observed compared with WT cells. This was consistent with the loss of assimilatory  $\text{NO}_3^-$  reductase expression, but not  $\text{NO}_2^-$  reductase expression, in *nasC* cells (Table 1). MV-NR activity could be restored to WT levels in the *nasC* mutant, when the deletion was complemented with a corresponding plasmid-borne gene copy. Also, MV-NIR activity was absent from the *nirA* mutant (Table 1), consistent with the loss of assimilatory  $\text{NO}_2^-$  reductase expression. However, the *nirA* mutant showed similar levels of MV-NR activity present in the parental strain following incubation with  $\text{NO}_3^-$ . Additional experiments revealed that MV-NR levels of *flp* cells showed an apparent ~2-fold increase in activity compared with WT incubation with  $\text{NO}_3^-$ , but MV-NIR activity was relatively similar in both *flp* and WT cells (Table 1). That the absence of Flp (i.e. the proposed electron donor and partner to NasC) should increase MV-NR activity may result from modulation in catalytic activity of the isolated NasC protein. Alternatively, without Flp, the artificial chemical electron donor could have greater access to NasC and thus may enhance  $\text{NO}_3^-$  reductase activity. Finally, as shown in Table 1, MV-NR and MV-NIR activities of *bjgb* or *narK* mutants were similar to those observed in WT cells.

### Regulation of the *narK-bjgb-flp-nasC* operon and *nirA* by NasS-NasT

In order to test the involvement of the NasT regulatory protein in  $\text{NO}_3^-$ -dependent induction of the *narK-bjgb-flp-nasC* operon and *nirA* gene, we examined expression of *narK-lacZ* and *nirA-lacZ* transcriptional fusion constructs in WT and *nasT* mutant cells following aerobic culture in the presence or absence of the inducer  $\text{NO}_3^-$  (Table 2). Whereas similar low levels of  $\beta$ -galactosidase activity were observed from both fusions in WT cells incubated without  $\text{NO}_3^-$ , the presence of this molecule induced expression of the *narK-lacZ* and *nirA-lacZ* transcriptional fusions by approximately 5- and 3-fold respectively. However,  $\beta$ -galactosidase activity from the *narK-lacZ* reporter was undetectable in the *nasT* strain regardless of whether  $\text{NO}_3^-$  was present or not (Table 2). Although similar basal levels of *nirA-lacZ* expression were observed in WT and *nasT* cells incubated without  $\text{NO}_3^-$ , a decrease of approximately 2-fold was found in *nasT* compared with WT when cells were incubated in the presence of  $\text{NO}_3^-$  (Table 2).

**Table 2**  $\beta$ -Galactosidase activity for *narK-lacZ* and *nirA-lacZ* fusions in *B. japonicum* WT, *nasS* or *nasT* strains

Cells were cultured under aerobic conditions, in minimal medium, with or without  $\text{NO}_3^-$  as sole N-source. Data are means  $\pm$  S.D. from at least three independent cultures, assayed in triplicate; n.d., not detectable.

<i>B. japonicum</i> str.	Relevant genotype	Miller units	
		$-\text{NO}_3^-$	$+\text{NO}_3^-$
4009	WT:: <i>narK-lacZ</i>	153 $\pm$ 40	759 $\pm$ 54
4012-4009	<i>nasS</i> :: <i>narK-lacZ</i>	972 $\pm$ 132	897 $\pm$ 66
4013-4009	<i>nasT</i> :: <i>narK-lacZ</i>	n.d.	n.d.
4018	WT:: <i>nirA-lacZ</i>	137 $\pm$ 22	395 $\pm$ 56
4012-4018	<i>nasS</i> :: <i>nirA-lacZ</i>	412 $\pm$ 37	372 $\pm$ 31
4013-4018	<i>nasT</i> :: <i>nirA-lacZ</i>	163 $\pm$ 34	203 $\pm$ 13

Additional studies to examine the role of NasS in NasT-dependent induction of the *narK-bjgb-flp-nasC* operon and *nirA* gene were also performed, using *narK-lacZ* or *nirA-lacZ* reporters. Here,  $\beta$ -galactosidase assays revealed that, in the absence of  $\text{NO}_3^-$ , the activity of each reporter fusion was significantly higher (approximately 6- and 3-fold for *narK-lacZ* and *nirA-lacZ* respectively) in *nasS* cells compared with WT cells (Table 2). These results imply that, in the absence of  $\text{NO}_3^-$ , NasS is a repressor of *narK-bjgb-flp-nasC* and *nirA* transcription. When equivalent experiments were performed in WT and *nasS* cells that had been pre-exposed to  $\text{NO}_3^-$ , expression levels for each reporter-fusion were very similar (Table 2).

Collectively, the reporter-fusion results suggest an inhibitory role for NasS in NasT-dependent induction of gene expression in *B. japonicum* and that  $\text{NO}_3^-$ -responsive control of both *narK-bjgb-flp-nasC* and *nirA* assimilatory gene expression is lost *in vivo* without NasS. This mode of regulation is analogous to  $\text{NO}_3^-/\text{NO}_2^-$ -responsive control of *nas* gene expression by NasS-NasT in the related  $\alpha$ -proteobacterium *P. denitrificans* [21].

### Involvement of Bjgb and Flp in nitrosative stress defence

A marked difference in growth between the *bjgb* mutant [ $\mu_{\text{max}}$  (app)  $\sim$  0.02  $\text{h}^{-1}$ , maximum  $D$  (at 600 nm) = 0.45  $\pm$  0.02] and WT strains [ $\mu_{\text{max}}$  (app)  $\sim$  0.04  $\text{h}^{-1}$ , maximum  $D$  (at 600 nm) = 0.61  $\pm$  0.03] was observed under anaerobic conditions, in minimal medium with  $\text{NO}_3^-$  as N-source (Figure 2B; Supplementary Table S3). By contrast, growth of the *bjgb* mutant and WT strains was similar under aerobic conditions (Figure 2A; Supplementary Table S3). These observations suggest that Bjgb has a key role *in vivo* for  $\text{NO}_3^-$  assimilation under anaerobic conditions, but not during aerobic growth. Anaerobic  $\text{NO}_3^-$  reduction is known to generate the potent cytotoxin NO, which requires NO-detoxification and nitrosative stress defence systems for bacterial survival [43,44]. To investigate the role of Bjgb in NO-metabolism, the nitrosative stress agent SNP was added (at 1 mM final concentration) to microaerobic *B. japonicum* cultures following growth in minimal medium with L-glutamate (BG) as sole N-source. Growth of WT cells was not significantly perturbed, whereas addition of SNP resulted in transient growth arrest of *bjgb* and *flp* strains that was restored after 24 h (Figure 5A). Perhaps most significantly, a *norC* or a *bjgb;norC* double mutant showed a substantially longer period of growth inhibition of approximately 7 days following addition

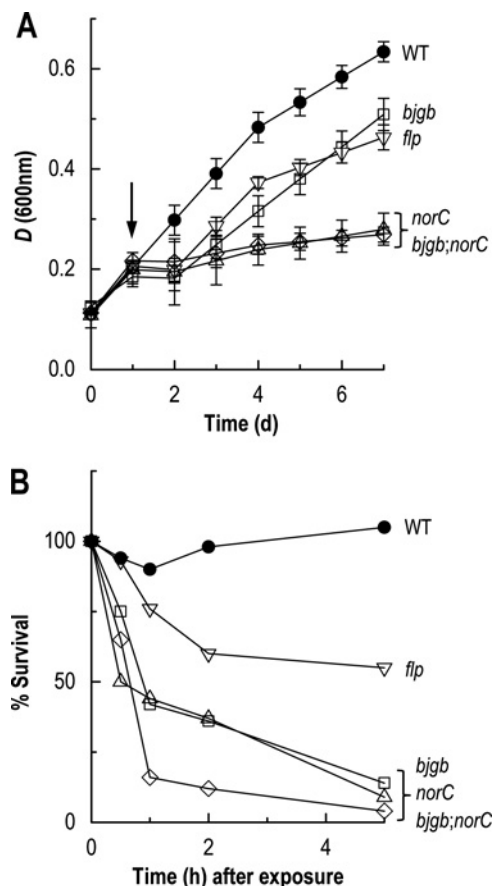


**Figure 5** Growth inhibition curves (A) and cell viability assays (B) for *B. japonicum* WT (●), *bjgb* (□), *flp* (▽), *norC* (△) and *bjgb;norC* (◇) strains in response to nitrosative stress induced by addition of SNP

For growth inhibition curves (A), *B. japonicum* strains were cultured microaerobically in BG minimal medium and 1 mM SNP was added after 1 d (as indicated by the arrow) and cell viability was measured from 1 to 5 h after exposure (B). The results presented are the mean of three biological replicates.

of SNP to cultures (Figure 5A). The effect of SNP on cell viability was also assayed by performing viable cell counts on samples taken at intervals spanning a 5-h period following addition of SNP to cultures. Although WT cell viability was not significantly affected, addition of SNP caused a  $\sim$ 60% decrease in cell survival for *norC* or *bjgb* cultures after 2 h (Figure 5B). The most prominent effect was observed with the *bjgb;norC* double mutant, which was the most sensitive to nitrosative stress. Here, approximately 80% of cells were killed within 1–2 h following SNP exposure (Figure 5B). Furthermore, the addition of SNP provoked a  $\sim$ 40% decrease in *flp* viability after 2 h incubation. These results revealed the importance of Bjgb and Flp for protection against nitrosative stress in *B. japonicum* under free-living conditions. NO is a product of SNP breakdown and a similar sensitivity of *bjgb* or *flp* mutants to NO was observed using spermine NONOate as an NO-generating compound (result not shown). Importantly, complementation with pDB4014 (harbouring a functional plasmid-borne copy of *bjgb*) allowed the *bjgb* mutant to grow anaerobically with  $\text{NO}_3^-$  to near WT levels (Supplementary Table S3). This confirmed that the growth phenotype observed for the *bjgb* mutant was not caused by a downstream effect on *flp* gene expression.



**Table 3** NO consumption activity and N<sub>2</sub>O levels for *B. japonicum* WT, *bjgb*, *flp*, *norC* and *bjgb;norC* strains cultured in BSN3 minimal medium under 2% (v/v) initial O<sub>2</sub>

Data are expressed as the means ± S.D. from at least two different cultures assayed in triplicate; n.d., not detectable.

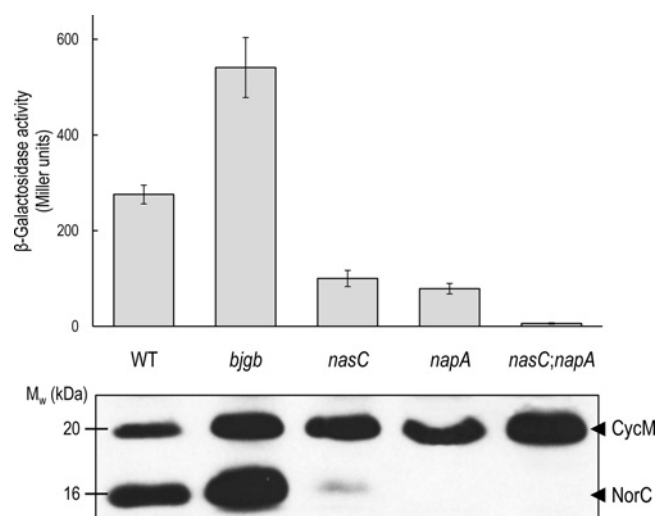
<i>B. japonicum</i> str.	Genotype	NO consumption activity (nmol · h <sup>-1</sup> · mg · protein <sup>-1</sup> )	N <sub>2</sub> O (mM)
USDA110	WT	155 ± 29	1.04 ± 0.26
4001	<i>bjgb</i>	384 ± 65	2.34 ± 0.16
4002	<i>flp</i>	101 ± 17	0.88 ± 0.03
GRC131	<i>norC</i>	97 ± 14	n.d.
GRC131-4001	<i>bjgb;norC</i>	92 ± 18	n.d.

### NO formed during NO<sub>3</sub><sup>-</sup> assimilation induces *nor* gene expression

To further investigate the role of Bjgb and Flp in NO metabolism, the ability of *B. japonicum* *bjgb* and *flp* strains to consume NO was analysed. Here, cells were incubated in BSN3 medium, with 2% initial O<sub>2</sub> and NO consumption rates were determined using an NO-electrode (Supplementary Figure S3). A ~2.5-fold increase in NO consumption was observed in the *bjgb* mutant compared with the WT strain (Table 3). This increase was not observed in the *flp* mutant, which showed NO consumption rates marginally lower than that observed in WT cells (Table 3; Supplementary Figure S3). NO consumption in the *norC* or the *bjgb;norC* mutants was approximately 1.6- and 1.7-fold lower respectively, compared with that observed in WT cells (Table 3; Supplementary Figure S3). The presence of residual activity in the *bjgb;norC* implies that under our experimental conditions, another enzyme(s) or perhaps a chemical process may be involved in NO consumption. The ability of *bjgb* cells to produce N<sub>2</sub>O following incubation in BSN3 medium with 2% initial O<sub>2</sub> was also investigated. The *bjgb* mutant produced approximately 2.5-fold more N<sub>2</sub>O than WT cells. By contrast, the level of N<sub>2</sub>O produced by the *flp* mutant was comparable to WT (Table 3). Given that N<sub>2</sub>O production was not detected for either the *norC* or the *bjgb;norC* mutants, this suggested the NorCB enzyme was the main source of N<sub>2</sub>O *in vivo*.

To test whether the higher levels of NO consumption and N<sub>2</sub>O production observed by the *bjgb* mutant were due to an induction of NorCB expression, *norC* transcription and relative abundance of NorC in membrane extracts were analysed, using a *norC-lacZ* transcriptional fusion and haem staining SDS-PAGE respectively. Firstly, a ~2-fold increase in *norC-lacZ* expression was observed in the *bjgb* mutant compared with WT (Figure 6). Given that the *norC* promoter is highly sensitive to N-oxides, including NO [31], an induction of β-galactosidase activity implies that Bjgb may act as a net sink for NO in WT cells. By contrast, β-galactosidase activity of the *norC-lacZ* transcriptional fusion was similar for both the *nasC* and the *napA* mutants, being approximately 3-fold lower compared with WT levels (Figure 6). Activity of the *norC-lacZ* transcriptional fusion was essentially abolished in the *nasC;napA* double mutant, implying that NO<sub>3</sub><sup>-</sup> reduction by NasC or NapA was the source of NO required for *norC-lacZ* expression (Figure 6).

SDS-PAGE analysis of membranes (that were normalized for total protein) by haem staining was used as a qualitative assay for expression of the NorC cytochrome. In *bjgb* cells, NorC levels were significantly increased relative to WT (Figure 6 inset; compare lanes 1 and 2). However, a clear decrease in NorC expression was observed in the *nasC* mutant compared with WT (Figure 6 inset; compare lanes 1 and 3). Furthermore, haem staining failed to detect NorC expression in membranes prepared

**Figure 6** Expression of *B. japonicum* *nor* genes during NO<sub>3</sub><sup>-</sup>-dependent growth

β-Galactosidase expression levels for the *norC-lacZ* transcriptional fusion in the WT, *bjgb*, *nasC*, *napA* and *nasC;napA* strains grown in BSN3 minimal medium containing 2% initial O<sub>2</sub> (v/v) and NO<sub>3</sub><sup>-</sup> as sole N-source. Haem-staining SDS-PAGE analysis of membrane fractions from *B. japonicum* strains is inset below. Each lane contains ~20 μg of total protein for the strains described. Haem-staining bands for previously identified c-type cytochromes, CycM and NorC, are indicated.

from either the *napA* or the *nasC;napA* mutant (Figure 6 inset; compare lane 1 with lane 4 or 5).

## DISCUSSION

### Defining the key components and transcriptional architecture of NO<sub>3</sub><sup>-</sup> and NO<sub>2</sub><sup>-</sup> assimilation in *B. japonicum*

A series of molecular genetics studies have established that genes encoded at two distinct loci, blr2806–09 and bli4571–73 of the *B. japonicum* genome (<http://genome.kazusa.or.jp/rhizobase/>), encode structural and regulatory components of a combined assimilatory NO<sub>3</sub><sup>-</sup> reductase and NO detoxification system (Figure 1). RT-PCR experiments demonstrate that the *nark-bjgb-flp-nasC* genes (present at blr2806–09 respectively) constitute a transcriptional unit. However, three putative genes (blr2803–05) predicted to encode a NO<sub>3</sub><sup>-</sup> transport system (similar to NrtABC, reviewed in [45]) and that lie immediately upstream of the *nark* operon are transcribed from a different promoter. The *nasTS-nirA* gene cluster (present at bli4571–73 respectively) lies some 2 Mb from the *nark* operon in the genome and encodes a NO<sub>3</sub><sup>-</sup>/NO<sub>2</sub><sup>-</sup> responsive two-component regulatory system, NasS-NasT [22] and a putative ferredoxin-dependent NO<sub>2</sub><sup>-</sup> reductase (NirA).

A role for the *bjgb* (blr2807) gene product in NO detoxification has been described [3,20], but the functions of other putative proteins encoded within the *nark* operon and biochemical components for the assimilatory NO<sub>3</sub><sup>-</sup> reductase pathway in *B. japonicum* were unknown. In the present work, we have demonstrated that the assimilatory NO<sub>3</sub><sup>-</sup> reductase (we rename herein as NasC) is encoded by blr2809 and is essential for NO<sub>3</sub><sup>-</sup>-dependent growth. The second core cytoplasmic enzyme component of the NO<sub>3</sub><sup>-</sup> assimilation pathway is NirA, which is required for growth on either NO<sub>3</sub><sup>-</sup> or NO<sub>2</sub><sup>-</sup> as sole N-source. Consistent with our findings, it has recently been demonstrated that NirA (encoded by bli4571) is required for utilization of

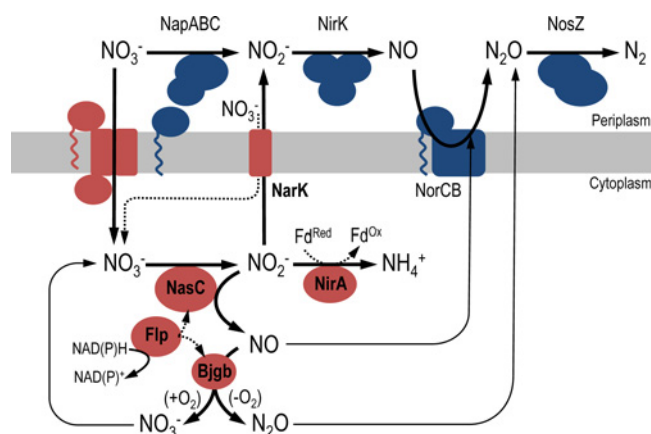


**Figure 7** Proposed biochemical pathway for  $\text{NO}_3^-$ -assimilation and NO-detoxification (red), alongside well-characterized systems for dissimilatory  $\text{NO}_3^-$  respiration (blue) in *B. japonicum*

Assimilatory reduction of  $\text{NO}_3^-$  to  $\text{NH}_4^+$  is performed by sequential action of the  $\text{NO}_3^-$ -reductase NasC and ferredoxin (Fd)-dependent  $\text{NO}_2^-$ -reductase NirA. Electrons from NAD(P)H are supplied to NasC and also Bjgb by Flp. During assimilatory  $\text{NO}_3^-$  reduction, cytoplasmic  $\text{NO}_2^-$  may accumulate and be further reduced, by NasC, to generate cytotoxic NO. NarK can counteract accumulation of  $\text{NO}_2^-$  by exporting it to the periplasm. Alternatively, Bjgb may detoxify the NO, formed by adventitious reduction in cytosolic  $\text{NO}_2^-$ , to  $\text{NO}_3^-$  or  $\text{N}_2\text{O}$  in the presence or absence of  $\text{O}_2$  respectively. Expression of NorCB is up-regulated during  $\text{NO}_3^-$  assimilation and this respiratory system may assist Bjgb to limit accumulation of NO and maintain cell viability.

$\text{NO}_3^-$  or  $\text{NO}_2^-$  as sole N-source in *B. japonicum* [46].  $\text{NO}_3^-$ -dependent induction of *nasC* (as part of the *narK* operon) and *nirA* expression is mediated by the two-component regulator NasS-NasT, an observation that is consistent with the role of this system in other  $\alpha$ -proteobacteria [21].

Phenotypic analyses of a mutant lacking Flp (encoded by *blr2808*) suggest that Flp mediates electron transfer to NasC, but not to NirA. Consecutive genes from the same operon encode Flp and NasC, but lie in a different genetic locus to *blr4571* (*nirA*). This genetic organization may explain the requirement of Flp for  $\text{NO}_3^-$  assimilation but not for  $\text{NO}_2^-$  assimilation, which instead is ferredoxin dependent (Figure 7). In contrast with *B. japonicum*, in *P. denitrificans* the regulatory and structural elements for a cytoplasmic  $\text{NO}_3^-/\text{NO}_2^-$  reductase system comprise a large gene cluster, *nasTSABGHC* [23]. The absence of a *nasG* homologue in either the *narK* operon or the *nirA* cluster in *B. japonicum* is notable. NasG may mediate electron flux to both the  $\text{NO}_3^-$  reductase and the  $\text{NO}_2^-$  reductase in other bacteria to prevent accumulation of excess  $\text{NO}_2^-$  by  $\text{NO}_3^-$  reduction in the cytoplasmic compartment [23,25]. Instead, for *B. japonicum*, genes encoding systems for  $\text{NO}_2^-$  transport and NO-detoxification are present within the operon encoding the  $\text{NO}_3^-$  reductase, which generates  $\text{NO}_2^-$ .

Sequence comparison of *blr2806* with homologous proteins from diverse bacterial phyla suggests that this gene encodes an MFS-type  $\text{NO}_3^-/\text{NO}_2^-$  antiporter with similarity to *E. coli* NarK. The capacity of a *B. japonicum narK* mutant to accumulate  $\text{NO}_2^-$  inside the cell demonstrates the involvement of NarK in  $\text{NO}_2^-$  export. Further, phenotypic analyses reveal that NarK is not the main system for cytoplasmic  $\text{NO}_3^-$  import, as *narK* cells were still able to grow on  $\text{NO}_3^-$ . Instead, the *narK* mutant showed enhanced growth compared to WT cells with  $\text{NO}_3^-$  as sole N-source, either under aerobic or anaerobic conditions. These observations imply that NarK acts to lower cytoplasmic  $\text{NO}_2^-$  levels by exporting  $\text{NO}_2^-$  to the periplasm and this process may

involve corresponding import of  $\text{NO}_3^-$  (Figure 7) [40]. In this respect, it is significant that *B. japonicum* NarK performs a very different role to the MFS-type  $\text{NO}_3^-/\text{NO}_2^-$  transporter NasA, which supplies  $\text{NO}_3^-$  to the cytoplasmic  $\text{NO}_3^-/\text{NO}_2^-$  reductase pathway in other  $\alpha$ -proteobacteria [23]. Instead, by counteracting  $\text{NO}_2^-$  accumulation, the *B. japonicum* NarK protein may thus represent a first level of protection to mitigate the production of cytotoxic NO, by adventitious reduction of  $\text{NO}_2^-$  within the cytoplasm [43]. However, as a consequence, in WT cells NarK may also lower substrate availability for NirA and thus limit growth on  $\text{NO}_3^-$ .

Deletion of *blr2803–05* that bioinformatics analyses had predicted to collectively encode an NrtABC family transporter, did not affect the ability of *B. japonicum* to assimilate  $\text{NO}_3^-$  as sole N-source. Therefore, the main route(s) for assimilatory  $\text{NO}_3^-$  import remains to be established. Although *blr2803–05* are not required for  $\text{NO}_3^-$  assimilation, there are other NtrABC-like candidates present on the chromosome (e.g. *blr5732–34*) that may facilitate  $\text{NO}_3^-$  import to the cytoplasm.

### A modular detoxification system for NO generated during $\text{NO}_3^-$ assimilation

In general, Nas systems have a high degree of structural plasticity, yet most contain proteins for transport and reduction of  $\text{NO}_3^-$  and  $\text{NO}_2^-$  [23,25,45,47,48]. In the present work, a novel  $\text{NO}_3^-$  assimilation system that also includes proteins for NO-detoxification is reported. The *narK-bjgb-flp-nasC* operon in *B. japonicum* encodes the sdHb Bjgb [3,20], which is homologous to the N-terminal haem-containing domain of *E. coli* FHb (Hmp) as well as the sdHbs from *Vitreoscilla stercoraria* (Vgb) and *Campilobacter jejuni* (Cgb) [20].

Deletion of *bjgb* had a strong negative affect on  $\text{O}_2$ -limited growth with  $\text{NO}_3^-$  as sole N-source, relative to WT, which implies a role for Bjgb in protecting *B. japonicum* cells from nitrosative stress. Importantly, in the absence of Bjgb,  $\text{NO}_3^-$  respiring cells were also highly sensitive to exogenous NO. Since growth of the *bjgb* mutant was not affected under aerobic conditions, the role of Bjgb may be restricted to anaerobic  $\text{NO}_3^-$ -dependent growth. However, our data suggest that the contribution of Bjgb to  $\text{N}_2\text{O}$  production *in vivo* is low. These observations are consistent with studies performed in *E. coli*, which reveal Hmp can reduce NO to  $\text{N}_2\text{O}$  under anaerobic conditions, but with a much lower rate compared with the activity of the FIRd NorV [44]. Furthermore, expression of the respiratory NorCB is significantly up-regulated in the *bjgb* mutant, relative to WT (see Figure 6), in response to increased intracellular NO levels that arise during  $\text{NO}_3^-$ -dependent growth. This result suggests that increased NorCB expression may counteract accumulation of cytotoxic NO and may partially compensate for the absence of the cytoplasmic Bjgb NO-detoxification system to maintain cell viability, albeit with a detrimental impact on anaerobic growth. Consequently, the bulk of the  $\text{N}_2\text{O}$  produced by the *bjgb* mutant can be attributed to NorCB activity, which is increased by  $\sim 2$ -fold relative to WT levels.

In *E. coli* Hmp, the FAD prosthetic group within the C-terminal NADH-reductase domain provides electrons from NAD(P)H that are required to reduce the NO-bound haem active site and complete the catalytic cycle. Aside from NO dioxygenation, Hmp has also been shown to perform slower reduction of NO to  $\text{N}_2\text{O}$  under anoxic conditions, which operates at approximately 1% of the rate observed for aerobic dioxygenase activity [49–52]. In the case of Cgb (an sdHb family protein that like Bjgb lacks the reductase domain present in the FHb Hmp), the electron-donor

protein remains to be identified. However, recent heterologous expression studies of Cgb in *E. coli* have reported a minor role for the NADH-(flavo)rubredoxin oxidoreductase NorW [53]. In *B. japonicum*, the enhanced sensitivity of the *flp* mutant to chemical NO-donors suggests that Flp may supply electrons from NAD(P)H that are required for Bjgb activity (Figure 7).

### Sources of NO: NasC and NapA activity is responsible for elevated NorCB expression

In eukaryotes, NO synthase (NOS) enzymes have been well described as the main NO-forming pathway for cell signalling and anti-microbial host defence [54]. By contrast, NO-formation in prokaryotes has been considered a by-product of denitrification, anaerobic ammonium oxidation and other related respiratory pathways [55–58]. However, NO is now increasingly recognized as a key substrate for ‘non-respiratory’ pathways in bacteria, e.g. those that protect against nitrosative stress and the link between NO-detoxification and pathogenicity has been the focus of several studies (reviewed by Maia and Moura [56,59]). The biochemical basis for NO-formation during anaerobic bacterial respiration has been shown to result from enzymic reduction of the pseudo-substrate  $\text{NO}_2^-$  by the respiratory membrane-bound  $\text{NO}_3^-$  reductase, Nar [43,60,61]. Furthermore, a small contribution (less than 3%) has been attributed to the periplasmic enzyme, Nap [43,61]. In the context of this present study, the potential contribution of cytoplasmic  $\text{NO}_2^-$  reduction to NO formation, by NasC, during  $\text{NO}_3^-/\text{NO}_2^-$  assimilation has not yet been investigated.

In the denitrifying endosymbiotic bacterium *B. japonicum*, reduction of  $\text{NO}_2^-$  by the periplasmic copper-dependent  $\text{NO}_2^-$  reductase NirK is the main NO-forming process, which occurs during anaerobic  $\text{NO}_3^-$  respiration [1,42]. Many studies have proposed that NO activates transcription of *nor* genes and that this control is mediated by regulatory proteins designated NNR/NnrR and DNR (reviewed by Spiro [18,62]). In the present study, we demonstrate that cells lacking the periplasmic respiratory  $\text{NO}_3^-$  reductase NapA, where NO synthesis from denitrification is blocked, results in very low expression of NorCB. Perhaps our most important finding was that, in addition to NapA, the assimilatory  $\text{NO}_3^-$  reductase (NasC) is also responsible for generating NO, as induction of NorCB was significantly lowered and completely abolished, relative to WT, in the *nasC* and *nasC;napA* mutant strains respectively (Figure 6). Therefore, the importance of NasC not only in  $\text{NO}_3^-$  assimilation but also in NO production has been demonstrated.

Co-expression of *bjgb*, *flp* and *nasC* that constitute a combined  $\text{NO}_3^-$  assimilation/NO-detoxification system may represent a novel method by which bacteria maintain cytoplasmic NO homeostasis and protect against nitrosative stress imposed during  $\text{NO}_3^-$ -dependent growth, where pathways for both respiratory denitrification and  $\text{NO}_3^-/\text{NO}_2^-$  assimilation are active (Figure 7). Although co-regulation between similar NO-forming and consuming systems has been proposed in *Aspergillus nidulans* [63], to our knowledge, this is the first time where this mechanism has been reported in bacteria. Finally, should production of NO exceed concentrations that can be contained by Bjgb-Flp, a ‘safety’ mechanism exists to enhance expression of NorCB to drive reduction of excess NO to  $\text{N}_2\text{O}$ .

### AUTHOR CONTRIBUTION

Juan Cabrera, Ana Salas, María Torres, Eulogio Bedmar, David Richardson, Andrew Gates and María Delgado designed the research. Juan Cabrera, Ana Salas, María Torres,

Andrew Gates and María Delgado performed the research. Juan Cabrera, Ana Salas, David Richardson, Andrew Gates and María Delgado analysed the data. Andrew Gates and María Delgado wrote the manuscript.

### ACKNOWLEDGEMENTS

We thank Dr Hans-Martin Fischer (Institute of Microbiology, ETH Zürich, Switzerland) for providing the pSUP3535 plasmid.

### FUNDING

This work was supported by European Regional Development Fund (ERDF) co-financed grants from Ministerio de Economía y Competitividad, Spain [grant numbers: AGL2010-18607 and AGL2013-45087-R (to M.J.D.)]; the Junta de Andalucía [grant number PE2012-AGR1968 (to E.J.B.)]; the Biotechnology and Biological Sciences Research Council [grant number BB/M00256X/1 (to A.J.G.)]; and the Royal Society International Exchanges Programme, U.K. [grant number IE140222 (to A.J.G. and M.J.D.)]. J.J.C. was supported by a fellowship from the Consejo Superior de Investigaciones Científicas (CSIC) JAE programme. D.J.R. is a Royal Society Wolfson Foundation Merit Award holder.

### REFERENCES

- 1 Bedmar, E.J., Robles, E.F. and Delgado, M.J. (2005) The complete denitrification pathway of the symbiotic, nitrogen-fixing bacterium *Bradyrhizobium japonicum*. *Biochem. Soc. Trans.* **33**, 141–144 [CrossRef PubMed](#)
- 2 Delgado, M.J., Casella, S. and Bedmar, E.J. (2007) Denitrification in rhizobia-legume symbiosis. In *Biology of the Nitrogen Cycle* (Bothe, H., Ferguson, S.J. and Newton, W.E., eds), pp. 57–66, Elsevier, Amsterdam
- 3 Sánchez, C., Cabrera, J.J., Gates, A.J., Bedmar, E.J., Richardson, D.J. and Delgado, M.J. (2011) Nitric oxide detoxification in the rhizobia-legume symbiosis. *Biochem. Soc. Trans.* **39**, 184–188 [CrossRef PubMed](#)
- 4 Bedmar, E.J., Bueno, E., Correa, D., Torres, M.J., Delgado, M.J. and Mesa, S. (2013) Ecology of denitrification in soils and plant-associated bacteria. In *Beneficial Plant-Microbial Interactions: Ecology and Applications* (González, M.B.R. and González-López, J., eds), pp. 164–182, CRC Press, Florida
- 5 Horchani, F., Prévot, M., Boscari, A., Evangelisti, E., Meilhoc, E., Bruand, C., Raymond, P., Boncompagni, E., Aschi-Smiti, S., Puppo, A. and Brouquisse, R. (2011) Both plant and bacterial nitrate reductases contribute to nitric oxide production in *Medicago truncatula* nitrogen-fixing nodules. *Plant Physiol.* **155**, 1023–1036 [CrossRef PubMed](#)
- 6 Inaba, S., Ikenishi, F., Itakura, M., Kikuchi, M., Eda, S., Chiba, N., Katsuyama, C., Suwa, Y., Mitsui, H. and Minamisawa, K. (2012)  $\text{N}_2\text{O}$  emission from degraded soybean nodules depends on denitrification by *Bradyrhizobium japonicum* and other microbes in the rhizosphere. *Microbes Environ.* **27**, 470–476 [CrossRef PubMed](#)
- 7 Meakin, G.E., Bueno, E., Jepson, B., Bedmar, E.J., Richardson, D.J. and Delgado, M.J. (2007) The contribution of bacteroidal nitrate and nitrite reduction to the formation of nitrosylhaemoglobin complexes in soybean root nodules. *Microbiology* **153**, 411–419 [CrossRef PubMed](#)
- 8 Sánchez, C., Gates, A.J., Meakin, G.E., Uchiumi, T., Girard, L., Richardson, D.J., Bedmar, E.J. and Delgado, M.J. (2010) Production of nitric oxide and nitrosylhaemoglobin complexes in soybean nodules in response to flooding. *Mol. Plant Microbe Interact.* **23**, 702–711 [CrossRef PubMed](#)
- 9 Bates, B.C., Kundzewicz, S., Wu, J. and Palutikof, P. (2008) Climate change and water. In *Technical Paper of the Intergovernmental Panel on Climate Change*, p. 210, IPCC Secretariat, Geneva
- 10 Crutzen, P.J., Mosier, A.R., Smith, K.A. and Winiwarer, W. (2008)  $\text{N}_2\text{O}$  release from agro-biofuel production negates global warming reduction by replacing fossil fuels. *Atmos. Chem. Phys.* **8**, 389–395 [CrossRef](#)
- 11 Ravishankara, A.R., Daniel, J.S. and Portmann, R.W. (2009) Nitrous oxide ( $\text{N}_2\text{O}$ ): The dominant ozone-depleting substance emitted in the 21st century. *Science* **326**, 123–125 [CrossRef PubMed](#)
- 12 Kato, K., Kanahama, K. and Kanayama, Y. (2010) Involvement of nitric oxide in the inhibition of nitrogenase activity by nitrate in *Lotus* root nodules. *J. Plant Physiol.* **167**, 238–241 [CrossRef PubMed](#)
- 13 Meakin, G.E., Jepson, B.J., Richardson, D.J., Bedmar, E.J. and Delgado, M.J. (2006) The role of *Bradyrhizobium japonicum* nitric oxide reductase in nitric oxide detoxification in soya bean root nodules. *Biochem. Soc. Trans.* **34**, 195–196 [CrossRef PubMed](#)
- 14 Mills, P.C., Rowley, G., Spiro, S., Hinton, J.C. and Richardson, D.J. (2008) A combination of cytochrome *c* nitrite reductase (NrfA) and flavorubredoxin (NorV) protects *Salmonella enterica* serovar Typhimurium against killing by NO in anoxic environments. *Microbiology* **154**, 1218–1228 [CrossRef PubMed](#)

- 15 Pittman, M.S., Elvers, K.T., Lee, L., Jones, M.A., Poole, R.K., Park, S.F. and Kelly, D.J. (2007) Growth of *Campylobacter jejuni* on nitrate and nitrite: electron transport to NapA and NrfA via NrfH and distinct roles for NrfA and the globin Cgb in protection against nitrosative stress. *Mol. Microbiol.* **63**, 575–590 [CrossRef PubMed](#)
- 16 Poole, R.K. (2005) Nitric oxide and nitrosative stress tolerance in bacteria. *Biochem. Soc. Trans.* **33**, 176–180 [CrossRef PubMed](#)
- 17 Pullan, S.T., Monk, C.E., Lee, L. and Poole, R.K. (2008) Microbial responses to nitric oxide and nitrosative stress: growth, “omic,” and physiological methods. *Methods Enzymol.* **437**, 499–519 [CrossRef PubMed](#)
- 18 Spiro, S. (2011) Nitric oxide metabolism: physiology and regulatory mechanisms. In *Nitrogen Cycling in Bacteria: Molecular Analysis* (Moir, J.W.B., ed.), pp. 177–196. Caister Academic Press, Norfolk
- 19 Kaneko, T., Nakamura, Y., Sato, S., Minamisawa, K., Uchiyama, T., Sasamoto, S., Watanabe, A., Idesawa, K., Iriguchi, M., Kawashima, K. et al. (2002) Complete genomic sequence of nitrogen-fixing symbiotic bacterium *Bradyrhizobium japonicum* USDA110. *DNA Res.* **9**, 189–197 [CrossRef PubMed](#)
- 20 Cabrera, J.J., Sánchez, C., Gates, A.J., Bedmar, E.J., Mesa, S., Richardson, D.J. and Delgado, M.J. (2011) The nitric oxide response in plant-associated endosymbiotic bacteria. *Biochem. Soc. Trans.* **39**, 1880–1885 [CrossRef PubMed](#)
- 21 Luque-Almagro, V.M., Lyall, V.J., Ferguson, S.J., Roldán, M.D., Richardson, D.J. and Gates, A.J. (2013) Nitrogen oxygen-dependent dissociation of a two-component complex that regulates bacterial nitrate assimilation. *J. Biol. Chem.* **288**, 29692–29702 [CrossRef PubMed](#)
- 22 Sánchez, C., Itakura, M., Okubo, T., Matsumoto, T., Yoshikawa, H., Gotoh, A., Hidaka, M., Uchida, T. and Minamisawa, K. (2014) The nitrate-sensing NasST system regulates nitrous oxide reductase and periplasmic nitrate reductase in *Bradyrhizobium japonicum*. *Environ. Microbiol.* **16**, 3263–3274 [CrossRef PubMed](#)
- 23 Gates, A.J., Luque-Almagro, V.M., Goddard, A.D., Ferguson, S.J., Roldán, M.D. and Richardson, D.J. (2011) A composite biochemical system for bacterial nitrate and nitrite assimilation as exemplified by *Paracoccus denitrificans*. *Biochem. J.* **435**, 743–753 [CrossRef PubMed](#)
- 24 Pino, C., Olmo-Mira, F., Cabello, P., Martínez-Luque, M., Castillo, F., Roldán, M.D. and Moreno-Vivián, C. (2006) The assimilatory nitrate reduction system of the phototrophic bacterium *Rhodospirillum rubrum* E1F1. *Biochem. Soc. Trans.* **34**, 127–129 [CrossRef PubMed](#)
- 25 Luque-Almagro, V.M., Gates, A.J., Moreno-Vivián, C., Ferguson, S.J., Richardson, D.J. and Roldán, M.D. (2011) Bacterial nitrate assimilation: gene distribution and regulation. *Biochem. Soc. Trans.* **39**, 1838–1843 [CrossRef PubMed](#)
- 26 Delgado, M.J., Bonnard, N., Tresierra-Ayala, A., Bedmar, E.J. and Muller, P. (2003) The *Bradyrhizobium japonicum* napEDABC genes encoding the periplasmic nitrate reductase are essential for nitrate respiration. *Microbiology* **149**, 3395–3403 [CrossRef PubMed](#)
- 27 Robles, E.F., Sanchez, C., Bonnard, N., Delgado, M.J. and Bedmar, E.J. (2006) The *Bradyrhizobium japonicum* napEDABC genes are controlled by the FixLJ-FixK<sub>2</sub>-NnrR regulatory cascade. *Biochem. Soc. Trans.* **34**, 108–110 [CrossRef PubMed](#)
- 28 Regensburger, B. and Hennecke, H. (1983) RNA polymerase from *Rhizobium japonicum*. *Arch. Microbiol.* **135**, 103–109 [CrossRef PubMed](#)
- 29 Bergersen, F.J. (1977) A treatise on dinitrogen fixation. In *Biology: Section III* (Hardy, R.W. and Silver, W., eds), pp. 519–556. John Wiley & Sons, New York
- 30 Torres, M.J., Argandoña, M., Vargas, C., Bedmar, E.J., Fischer, H.M., Mesa, S. and Delgado, M.J. (2014) The global response regulator RegR controls expression of denitrification genes in *Bradyrhizobium japonicum*. *PLoS One* **9**, e99011 [CrossRef PubMed](#)
- 31 Torres, M.J., Bueno, E., Mesa, S., Bedmar, E.J. and Delgado, M.J. (2011) Emerging complexity in the denitrification regulatory network of *Bradyrhizobium japonicum*. *Biochem. Soc. Trans.* **39**, 284–288 [CrossRef PubMed](#)
- 32 Sambrook, J. and Russell, D. (2001) *Molecular Cloning: A Laboratory Manual*. Cold Spring Harbor, New York
- 33 Simon, R., Priefer, U. and Pühler, A. (1983) Vector plasmids for in-vivo and in-vitro manipulation of gram-negative bacteria. In *Molecular genetics of the bacteria-plant interaction* (Pühler, A., ed.), pp. 98–106. Springer-Verlag, Berlin [CrossRef](#)
- 34 Mesa, S., Velasco, L., Manzanera, M.E., Delgado, M.J. and Bedmar, E.J. (2002) Characterization of the *norCBQD* genes, encoding nitric oxide reductase, in the nitrogen fixing bacterium *Bradyrhizobium japonicum*. *Microbiology* **148**, 3553–3560 [CrossRef PubMed](#)
- 35 Egelhoff, T.T., Fisher, R.F., Jacobs, T.W., Mulligan, J.T. and Long, S.R. (1985) Nucleotide sequence of *Rhizobium meliloti* 1021 nodulation genes: *nodD* is read divergently from *nodABC*. *DNA* **4**, 241–248 [CrossRef PubMed](#)
- 36 Hauser, F., Pessi, G., Friberg, M., Weber, C., Rusca, N., Lindemann, A., Fischer, H.M. and Hennecke, H. (2007) Dissection of the *Bradyrhizobium japonicum* NifA +  $\sigma^{54}$  regulon, and identification of a ferredoxin gene (*fdxN*) for symbiotic nitrogen fixation. *Mol. Genet. Genomics* **278**, 255–271 [CrossRef PubMed](#)
- 37 Miller, J.H. (1972) *Experiments in Molecular Genetics*. Cold Spring Harbor, New York
- 38 Vargas, C., McEwan, A.G. and Downie, J.A. (1993) Detection of c-type cytochromes using enhanced chemiluminescence. *Anal. Biochem.* **209**, 323–326 [CrossRef PubMed](#)
- 39 Nicholas, D.J.D. and Nason, A. (1957) Determination of nitrate and nitrite. In *Methods in Enzymology* (Colowick, S.P. and Kaplan, N.O., eds), pp. 981–984. Academic Press, New York [CrossRef](#)
- 40 Fukuda, M., Takeda, H., Kato, H.E., Doki, S., Ito, K., Maturana, A.D., Ishitani, R. and Nureki, O. (2015) Structural basis for dynamic mechanism of nitrate/nitrite antiport by NarK. *Nat. Commun.* **6**, 7097 [CrossRef PubMed](#)
- 41 Goddard, A.D., Moir, J.W., Richardson, D.J. and Ferguson, S.J. (2008) Interdependence of two NarK domains in a fused nitrate/nitrite transporter. *Mol. Microbiol.* **70**, 667–681 [CrossRef PubMed](#)
- 42 Velasco, L., Mesa, S., Delgado, M.J. and Bedmar, E.J. (2001) Characterization of the *nirK* gene encoding the respiratory, Cu-containing nitrite reductase of *Bradyrhizobium japonicum*. *Biochim. Biophys. Acta* **1521**, 130–134 [CrossRef PubMed](#)
- 43 Rowley, G., Hensen, D., Felgate, H., Arkenberg, A., Appia-Ayme, C., Prior, K., Harrington, C., Field, S.J., Butt, J.N., Baggs, E. and Richardson, D.J. (2012) Resolving the contributions of the membrane-bound and periplasmic nitrate reductase systems to nitric oxide and nitrous oxide production in *Salmonella enterica* serovar Typhimurium. *Biochem. J.* **441**, 755–762 [CrossRef PubMed](#)
- 44 Vine, C.E. and Cole, J.A. (2011) Nitrosative stress in *Escherichia coli*: reduction of nitric oxide. *Biochem. Soc. Trans.* **39**, 213–215 [CrossRef PubMed](#)
- 45 Moreno-Vivián, C. and Flores, E. (2007) Nitrate assimilation in bacteria. In *Biology of the Nitrogen Cycle* (Bothe, H., Ferguson, S.J. and Newton, W.E., eds), pp. 263–292. Elsevier, Amsterdam [CrossRef](#)
- 46 Franck, W.L., Qiu, J., Lee, H.I., Chang, W.S. and Stacey, G. (2015) DNA microarray-based identification of genes regulated by NtrC in *Bradyrhizobium japonicum*. *Appl. Environ. Microbiol.* **81**, 5299–5308 [CrossRef PubMed](#)
- 47 Lin, J.T. and Stewart, V. (1998) Nitrate assimilation by bacteria. *Adv. Microb. Physiol.* **39**, 379 [PubMed](#)
- 48 Moreno-Vivián, C., Luque-Almagro, V.M., Cabello, P., Roldán, M.D. and Castillo, F. (2011) Transport and assimilation of inorganic nitrogen in bacteria. In *Nitrogen Cycling in Bacteria* (Moir, J.W.B., ed.), pp. 101–122. Caister Academic Press, Norfolk
- 49 Angelo, M., Hausladen, A., Singel, D.J. and Stamler, J.S. (2008) Interactions of NO with hemoglobin: from microbes to man. *Methods Enzymol.* **436**, 131–168 [CrossRef PubMed](#)
- 50 Gardner, P.R. (2005) Nitric oxide dioxygenase function and mechanism of flavohemoglobin, hemoglobin, myoglobin and their associated reductases. *J. Inorg. Biochem.* **99**, 247–266 [CrossRef PubMed](#)
- 51 Hernández-Urzúa, E., Mills, C.E., White, G.P., Contreras-Zentella, M.L., Escamilla, E., Vasudevan, S.G., Membrillo-Hernández, J. and Poole, R.K. (2003) Flavohemoglobin Hmp, but not its individual domains, confers protection from respiratory inhibition by nitric oxide in *Escherichia coli*. *J. Biol. Chem.* **278**, 34975–34982 [CrossRef PubMed](#)
- 52 Kim, S.O., Orii, Y., Lloyd, D., Hughes, M.N. and Poole, R.K. (1999) Anoxic function for the *Escherichia coli* flavohaemoglobin (Hmp): reversible binding of nitric oxide and reduction to nitrous oxide. *FEBS Lett.* **445**, 389–394 [CrossRef PubMed](#)
- 53 Tinajero-Trejo, M., Vreugdenhil, A., Sedelnikova, S.E., Davidge, K.S. and Poole, R.K. (2013) Nitric oxide reactivities of the two globins of the foodborne pathogen *Campylobacter jejuni*: roles in protection from nitrosative stress and analysis of potential reductants. *Nitric Oxide* **34**, 65–75 [CrossRef PubMed](#)
- 54 Alderton, W.K., Cooper, C.E. and Knowles, R.G. (2001) Nitric oxide synthases: structure, function and inhibition. *Biochem. J.* **357**, 593–615 [CrossRef PubMed](#)
- 55 Kartal, B., van Niftrik, L., Keltjens, J.T., Op den Camp, H.J. and Jetten, M.S. (2012) Anammox-growth physiology, cell biology, and metabolism. *Adv. Microb. Physiol.* **60**, 211–262 [CrossRef PubMed](#)
- 56 Maia, L.B. and Moura, J.J. (2014) How biology handles nitrite. *Chem. Rev.* **114**, 5273–5357 [CrossRef PubMed](#)
- 57 Rinaldo, S. and Cutruzzola, F. (2007) Nitrate reductases in denitrification. In *Biology of the Nitrogen Cycle* (Bothe, H., Ferguson, S.J. and Newton, W.E., eds), pp. 37–55. Elsevier Science, Amsterdam [CrossRef](#)
- 58 Zumft, W.G. (1997) Cell biology and molecular basis of denitrification. *Microbiol. Mol. Biol. Rev.* **61**, 533–616 [PubMed](#)
- 59 Maia, L.B. and Moura, J.J. (2015) Nitrite reduction by molybdoenzymes: a new class of nitric oxide-forming nitrite reductases. *J. Biol. Inorg. Chem.* **20**, 403–433 [CrossRef PubMed](#)
- 60 Gilberthorpe, N.J. and Poole, R.K. (2008) Nitric oxide homeostasis in *Salmonella typhimurium*: roles of respiratory nitrate reductase and flavohemoglobin. *J. Biol. Chem.* **283**, 11146–11154 [CrossRef PubMed](#)
- 61 Vine, C.E., Purewal, S.K. and Cole, J.A. (2011) NsrR-dependent method for detecting nitric oxide accumulation in the *Escherichia coli* cytoplasm and enzymes involved in NO production. *FEMS Microbiol. Lett.* **325**, 108–114 [CrossRef PubMed](#)

- 62 Spiro, S. (2012) Nitrous oxide production and consumption: regulation of gene expression by gas-sensitive transcription factors. *Philos. Trans. R Soc. Lond. B Biol. Sci.* **367**, 1213–1225 [CrossRef](#) [PubMed](#)
- 63 Schinko, T., Berger, H., Lee, W., Gallmetzer, A., Pirker, K., Pachlinger, R., Buchner, I., Reichenauer, T., Guldener, U. and Strauss, J. (2010) Transcriptome analysis of nitrate assimilation in *Aspergillus nidulans* reveals connections to nitric oxide metabolism. *Mol. Microbiol.* **78**, 720–738 [CrossRef](#) [PubMed](#)

---

Received 7 August 2015/11 November 2015; accepted 12 November 2015  
Accepted Manuscript online 12 November 2015, doi:10.1042/BJ20150880